Dopaminergic modulation of short-term synaptic plasticity at striatal inhibitory synapses

Fatuel Tecuapetla, Luis Carrillo-Reid, José Bargas*, and Elvira Galarraga

Depto de Biofísica, Instituto de Fisiología Celular, Universidad Nacional Autónoma de México, P.O. Box 70-253, 04510 México D.F., México

Communicated by Ranulfo Romo, National Autonomous University of Mexico, Mexico City, Mexico, April 25, 2007 (received for review February 6, 2007)

Circuit properties, such as the selection of motor synergies, have been posited as relevant tasks for the recurrent inhibitory synapses between spiny projection neurons of the neostriatum, a nucleus of the basal ganglia participating in procedural learning and voluntary motor control. Here we show how the dopaminergic system regulates short-term plasticity (STP) in these synapses. STP is thought to endow neuronal circuits with computational powers such as gain control, filtering, and the emergence of transitory net states. But little is known about STP regulation. Employing unitary and population synaptic recordings, we observed that activation of dopamine receptors can modulate STP between spiny neurons. A D_1-class agonist enhances, whereas a D_2-class agonist decreases, short-term depression most probably by synaptic redistribution. Presynaptic receptors appear to be responsible for this modulation. In contrast, STP between fast-spiking interneurons and spiny projection neurons is largely unregulated despite expressing presynaptic receptors. Thus, the present experiments provide an explanation for dopamine actions at the circuit level: the control of STP between lateral connections of output neurons and the reorganization of the balance between different forms of inhibitory transmission. Theoretically, D_1 receptors would promote a sensitive, responsive state for temporal precision (dynamic component), whereas D_2 receptors would sense background activity (static component).

dopamine | neostriatum | recurrent inhibition | presynaptic receptors | basal ganglia

Synaptic strength within neuronal circuits is continuously modified because of short-term plasticity (STP) (1–5). STP bestows circuits with functional capabilities such as detection of sudden changes, filtering, and fidelity transfer (5–8). Short-term depression (STD) is a form of STP. STD gives networks dynamic gain-control and filtering capabilities that facilitate synchronization (5, 6, 9, 10). It is little known what variables regulate STD. Synaptic inhibition in the neostriatum (NSt) relies in part on the synapses that interconnect spiny projection neurons (SPNs) (11–18). Numerous functions of the NSt are thought to depend on this inhibition (12, 19–22), such as the selection and organization of learned motor synergies and contrast enhancement (20–25). Another form of neostriatal inhibition is due to local circuit fast-spiking (FS) interneurons (13, 14, 26–32). The inhibition from FS interneurons is stronger than that between SPNs (13, 14, 26–32). But inhibition between SPNs makes the majority of contacts (12, 28, 32). Both types of inhibition exhibit STD (13, 14). The hypothesis that the dopaminergic system modulates STD in these synapses was tested in this work.

Dopamine is an important transmitter in the NSt (24, 33). In its absence, the circuit functionally collapses, inducing the devastating signs of Parkinson's disease (34–36). Although pre- and postsynaptic actions of dopamine have been described (24, 32, 37, 38), a global action with a potential impact at the circuit level is not known. Here we show that STD between SPNs can be regulated by the dopaminergic system (6, 32, 39).

Results

Two Types of Inhibition. The inhibition between SPNs (SPN→SPN connection) and between FS interneurons and SPNs (FS→SPN connection) was investigated with dual recordings. Inhibitory postsynaptic currents (IPSCs) were obtained from either connection by depolarizing presynaptic SPN or FS neurons (Fig. 1 *B* and *C*). IPSCs between SPNs were also recorded after antidromic stimulation of striofugal axons at the globus pallidus (GP) (called the GP→NSt connection to avoid confusion) (Fig. 1*A*) (32, 40–42) in the presence of glutamate receptor blockers (10 μM CNQX plus 50 μM APV). These responses were sensitive to 10 μM bicuculline (Fig. 1*D*) and are called "population" responses because they probably arise from various presynaptic axons (42). In contrast, synaptic currents evoked with dual recordings are called "unitary" responses (Fig. 1 *B*, *C*, and *G–I*). Results were obtained from 14 unitary SPN→SPN connections of 106 dual recordings (≈13%) at distances <100 μm (Fig. 1 *F* and *G*). SPN→SPN IPSCs were blocked by 10 μM bicuculline (13, 14, 16). Thirteen unitary FS→SPN IPSCs of 24 dual recordings (55%) were also obtained and blocked by bicuculline (10 μM) (13, 14, 16, 28). Fig. 1 *E–G* illustrates averages of several (20–24) unitary IPSCs (average, black traces; individual trials, gray traces).

Evidence supporting that IPSCs recorded from GP→NSt connections are the "population" version (Fig. 1*E*) of the "unitary" IPSCs recorded from SPN→SPN connections (Fig. 1*F*) was found (32, 40–42). First, shape index plots (graphing half widths vs. rise times) of mean IPSCs (GP→NSt, empty circles; SPN→SPN, filled circles) showed no significant differences between these two connections (Fig. 1*H*; $n = 9$; NS; Mann–Whitney *U* test). This comparison had not been done before, and the result strongly confirms that field stimulation at the GP can isolate the synapses interconnecting SPNs. In contrast, comparison of the two unitary connections (Fig. 1 *F* and *G*; SPN→SPN, filled circles; FS→SPN, gray circles) showed significant differences for the same parameters (Fig. 1*I*). FS→SPN IPSCs had significantly faster rise and decay times. FS→SPN responses were stronger on average than SPN→SPN responses [56 ± 12 pA vs. 23 ± 4 pA, respectively; $P < 0.01$; Mann–Whitney *U* test; see supporting information (SI) *Text* for statistical details] (13, 14, 28, 32). Moreover, superimposition of normalized IPSCs showed identical time courses for GP→NSt and SPN→SPN connections (Fig. 1*J*), but significantly different shapes from IPSCs recorded from FS→SPN connections. However, despite having strong evidence that SPN→SPN unitary and GP→NSt population responses come from the same synapse, kinetics of their STP were also compared (during activation of

Author contributions: F.T., J.B., and E.G. designed research; F.T. and E.G. performed research; L.C.-R. contributed new reagents/analytic tools; F.T., L.C.-R., and J.B. analyzed data; and F.T., J.B., and E.G. wrote the paper.

The authors declare no conflict of interest.

Freely available online through the PNAS open access option.

Abbreviations: SPN, spiny projection neuron; FS, fast-spiking; GP, globus pallidus; NSt, neostriatum; IPSC, inhibitory postsynaptic current; STP, short-term plasticity; STD, short-term depression; CV, coefficient of variation.

*To whom correspondence should be addressed. E-mail: jbargas@ifc.unam.mx.

This article contains supporting information online at www.pnas.org/cgi/content/full/0703813104/DC1.

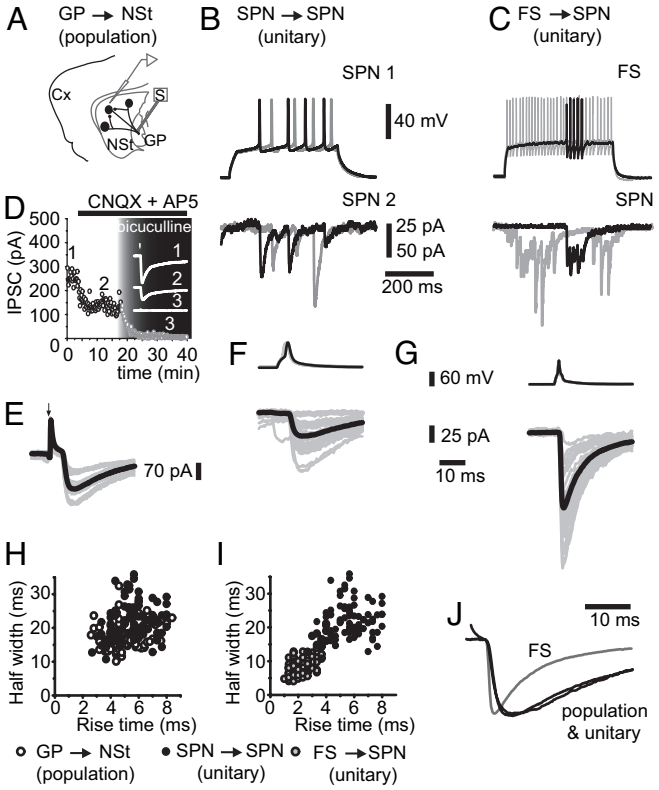

Fig. 1. Inhibition in the NSt. (*A*) Arrangement for recording ''population'' IPSCs from GP→NSt connections. A postsynaptic SPN of the NSt is being recorded. It receives multiple terminals from other SPNs. Striofugal axons from SPNs, which are presynaptic to the recorded SPN, are stimulated antidromically (S) at the GP. (*B*) SPN→SPN connection: Evoked action potentials (APs) in a presynaptic SPN (SPN1) generate IPSCs in a postsynaptic SPN (SPN2). (*C*) FS→SPN connection: Evoked APs in a presynaptic FS interneuron generate either tonic (gray) or bursting (black) discharges that evoke IPSCs in a postsynaptic SPN. (*D*) GP→NSt synaptic responses (1) are blocked by 10 μM CNQX and 50 μM APV, leaving an IPSC (2) that can be blocked by 10 μM bicuculline (3). (*E*) IPSC from the GP→NSt connection. Arrow, stimulus artifact; black trace, average of 20 of 24 individual responses (gray). (*F*) IPSC from the SPN→SPN connection. (*G*) IPSC from the FS→SPN connection. (*F* and *G Upper*) Traces of presynaptic APs. (*F* and *G Lower*) Unitary IPSCs. (*H*) IPSC rise times against half widths (shape index plots) obtained from GP→NSt (empty circles) and SPN→SPN (filled circles) connections (n = 9). Note that the samples are undistinguishable from each other. (*I*) Same plot comparing FS→SPN (gray circles) and SPN→SPN (filled circles) connections (n = 9). Note that the samples are clearly separate. (*J*) Averaged and normalized IPSCs from all three connections. Note virtual identical shapes for SPN→SPN (unitary) and GP→NSt (population) connections. Gray trace corresponds to the FS→SPN connection.

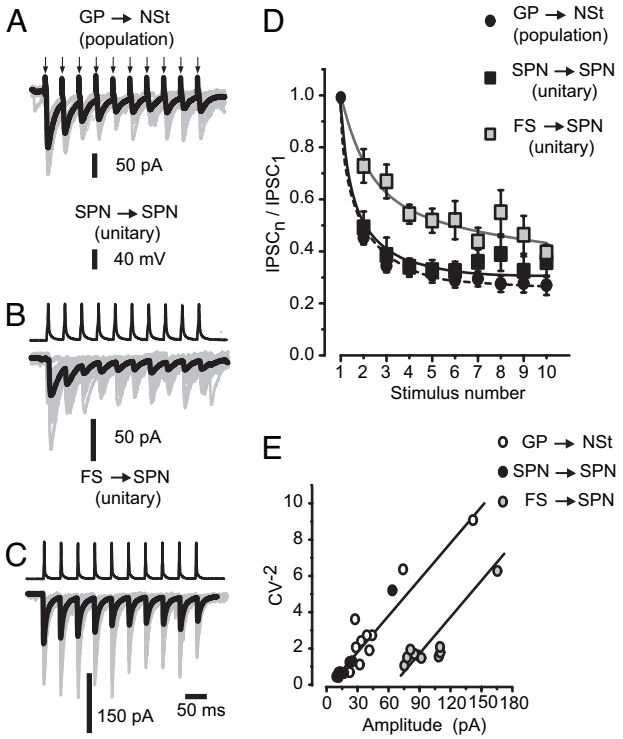

Fig. 2. STD kinetics of neostriatal inhibitory synapses. From top to bottom, trains of IPSCs from each connection in response to a 20-Hz train of stimulus delivered at 0.1 Hz. (*A*) GP→NST. (*B*) SPN→SPN. (*C*) FS→SPN. (*A–C*) Black trace, average of 25 individual responses (gray). (*D*) STD kinetics: Normalized and averaged IPSC amplitudes evoked with stimulus trains. Lines are fits to: $IPSC(t) = A_1e^{-x/\tau 1} + A_2e^{-x/\tau 2} + y0$, where τ_1 is the faster time constant of decay (see *Materials and Methods*). Note virtually identical STD kinetics for SPN→SPN (unitary) and GP→NSt (population) connections and a slower decay for the FS→SPN connection. (*E*) Direct relationships between IPSC amplitudes and CV^{-2} ($r^2 > 0.9$ for all connections; $P < 0.002$). Note the plot superimposition for SPN→SPN (unitary) and GP→NSt (population) connections and a separate relationship for the FS→SPN connection.

the GP→NSt connection, reciprocal inhibition between SPNs may alter subsequent responses in a train yielding spurious depression).

STP after trains of 10 stimuli delivered at 10, 20, and 50 Hz (Fig. 2 *A–C*) given at a low (0.1-Hz) frequency was studied. Fig. 2*D* illustrates that STP dynamics was virtually identical for GP→NSt and SPN→SPN connections, discarding that reciprocal inhibition interferes with plasticity (at least with this stimulation strength) and suggesting that presynaptic neurons impinging on the recorded neuron scarcely connect with each other. In contrast, STP in FS→SPN connections showed significant differences (Fig. 2*D*). These results validate the use of population responses (GP→NSt) to study STP in the synapses between SPNs. We chose responses to 20 Hz for most analyses because this frequency is commonly found in SPNs and corticostriatal afferents during behavioral tasks (43). Moreover, average interspike intervals during SPNs "up states" is ≈50 msec (≈20 Hz) (44). However, main results did not differ significantly at the other frequencies (13). STP for responses coming from all three connections was STD (13, 14). The STD ratio [mean amplitude of first IPSC divided over mean amplitude of last (7th to 10th) IPSCs] was 5.1 ± 0.4 (n = 27; median, 4.3; range, 1.1–20) for GP→NSt IPSCs and 4.5 ± 0.9 for SPN→ SPN IPSCs (n = 11; median, 3.0; range, 1.2–25) (NS; Kruskal–Wallis test; see *SI Text*), confirming that both protocols isolated the same synapse. In contrast, the STD ratio was significantly different for FS→SPN connections: 2.4 ± 0.2 (n = 10; median, 2.4; range, 0.9–4.0; $P < 0.01$). STD dynamics is peculiar to each class of synapse (1–4). By fitting a sum of exponential functions (2) to averaged and normalized STD plots (Fig. 2*D*), it was observed that the faster time constant (τ_1 of Eq. **1** in *Materials and Methods*) was larger for FS→SPN connections than for SPN→SPN connections (87 ± 11 msec vs. 31 ± 4 msec) ($P <$ 0.05). However, τ_1 of GP→NSt connections (31 ± 2 msec) was virtually identical to that from SPN→ SPN (NS). Furthermore, a significant correlation was found between IPSCs mean amplitude versus IPSCs reciprocal of the squared coefficient of variation (CV^{-2}), proportional to mean quantal content (Fig. 2*E*; n = 6 pairs for each input source), indicating that STD was greatly mediated by a presynaptic mechanism (r^2 of at least 0.9 ± 0.01; $P < 0.002$ for the three sources) (45). However, note that the correlations from GP→NSt and SPN→SPN synapses were undistinguishable from each other, whereas the correlation built from FS→SPN synapses was displaced to the right (Fig. 2*E*),

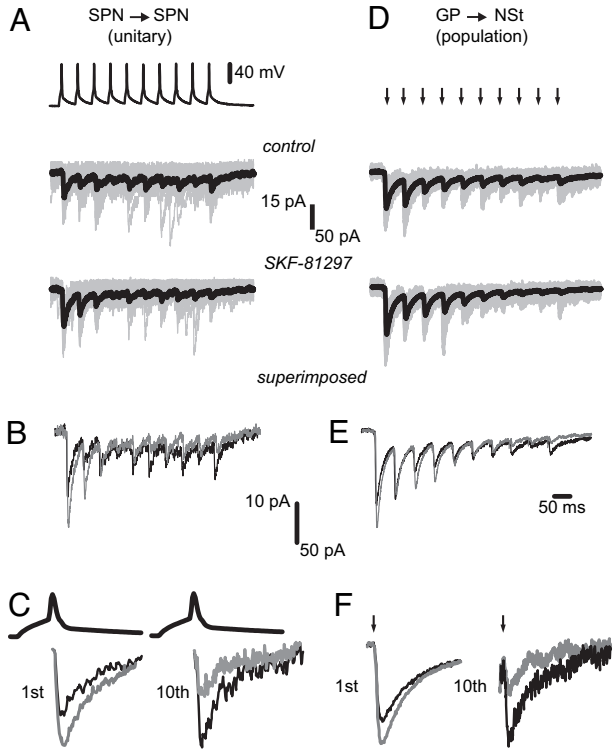

Fig. 3. D_1-class receptor activation enhances STD. (*A*) SPN→SPN connection. Presynaptic APs (*Top*), evoked IPSCs (*Middle*; average, black; trials, gray), and responses (*Bottom*) to the same stimuli after addition of SKF-81297 (1 μM). (*B*) Superimposition of average traces in control and after the D_1-agonist. (*C*) Amplification of the 1st and 10th responses at both conditions. (*D*) GP→NSt connection. From top to bottom, field stimuli at the GP (arrows) and evoked IPSCs in control and after addition of SKF-81297 (1 μM). (*E*) Superimposition of average traces in control and after the D_1-agonist. (*F*) Amplification of the 1st and 10th responses at both conditions. Note similarity of action of the D_1-agonist for unitary (*A–C*) and population (*D–F*) responses, the increase in the amplitude of $IPSC_1$, and the decrease in the paired pulse ratio ($IPSC_2/IPSC_1$) between the first two responses.

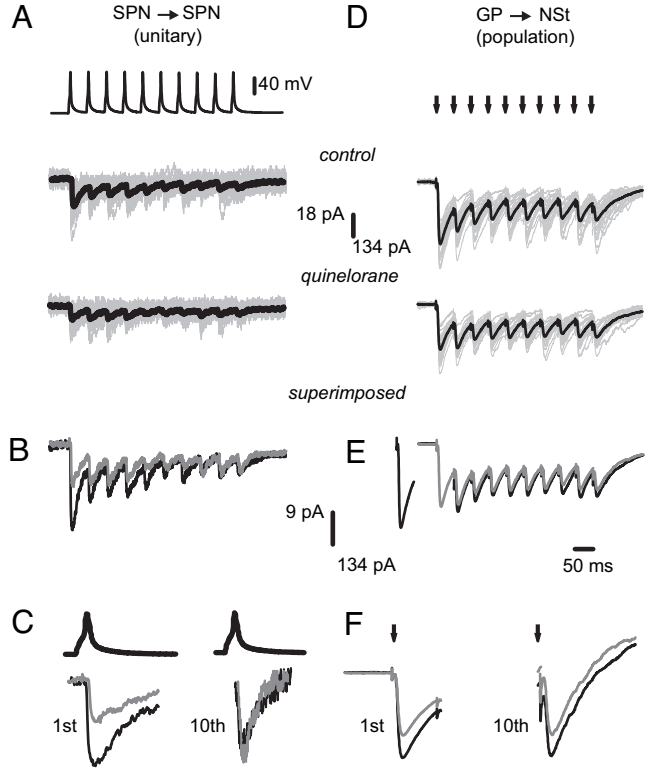

Fig. 4. D_2-class receptor activation decreases STD. (*A*) SPN→SPN connection. Presynaptic APs (*Top*), evoked IPSCs (*Middle*; average, black; trials, gray), and responses (*Bottom*) to the same stimuli after addition of quinelorane (1 μM). (*B*) Superimposition of average traces in control and after the D_2-agonist. (*C*) Amplification of the 1st and 10th responses at both conditions. (*D*) GP→NSt connection. Field stimuli at the GP (*Top*, arrows) and evoked IPSCs in control (*Middle*) and after (*Bottom*) addition of quinelorane (1 μM). (*E*) Superimposition of average traces in control and after the D_2-agonist. (*F*) Amplification of the 1st and 10th responses at both conditions. Note similarity of action of the D_2-agonist for unitary (*A–C*) and population (*D–F*) responses, the decrease in the amplitude of $IPSC_1$, and the increase in the paired pulse ratio for the first two IPSCs.

suggesting a greater quantal content for FS→ SPN synapses. In summary, half width, rise time, STD kinetics (τ1), and STD ratio strongly suggest that GP→ NSt and SPN→ SPN protocols isolate the same synapse: the one interconnecting SPNs. Further, this synapse has different functional characteristics than the FS→ SPN synapse, adding to previous evidence (32, 40–42). Therefore, if GP→ NSt and SPN→ SPN connections are two different ways to isolate the same synapse, a testable prediction is that the modulation induced by dopamine agonists should be the same for both responses. In this case, data from both experimental arrangements can be pooled together (population and unitary), yielding results with strong statistical value (unitary plus population).

STD Modulation in Synapses Between Spiny Neurons. Activation of D_1-class receptors during STD from SPN→SPN and GP→NSt connections (20-Hz trains) is shown in Fig. 3. The D_1-class selective agonist, SKF-81297 (1 μM), enhances STD for both SPN→SPN (n = 3 of 5 pair recordings) and GP→NSt (n = 5 of 12 population recordings) responses [n = 8 of 17 (47%) cases responded to D_1-agonist]. In the pool of responsive cases, the change in STD ratio was significant (mean ± SEM): 3.3 ± 0.4 before and 9.7 ± 3.7 after addition of SKF 81297 (n = 8; $P <$ 0.03). The fact that about half the cases did not respond to the D_1-agonist supports the hypothesis that dopamine receptors segregate in different sets of SPNs, at least at the level of synaptic terminals. STD enhancement was accompanied by an increase in the amplitude of the first response ($IPSC_1$) from 57 ± 17 pA before to 75 ± 20 pA after the D_1-agonist (n = 8; $P < 0.02$). To see whether this change was due to presynaptic mechanisms, the CV of $IPSC_1$ was assessed. It decreased for all D_1-responsive cases by 54 ± 8% ($P < 0.02$), suggesting mediation by presynaptic receptors (32). At the same time, a nonparametric test of variance rendered a significant increase in IPSC variance after SKF-81297 for each individual experiment (46) (n = 8; $P \leq 0.001$; F test), suggesting an increase in release probability for the first response (47). Finally, τ_1 of the STD process was significantly accelerated from 31 ± 3 to 23 ± 2 msec (n = 8; $P < 0.01$), showing that D_1-receptor activation accelerates STD kinetics. Taken together, changes in release probability and STD kinetics suggest synaptic "redistribution" (4, 8, 48). These actions were completely blocked by the selective D_1-receptor antagonist SCH 39393 (1 μM) (n = 4; data not shown). A selective (see *SI Text*) nonhydrolyzable D_1-class agonist (32, 37) was used for these experiments, and only stable responses at a train frequency of 0.1 Hz were chosen for analysis.

Activation of D_2-class receptors on SPN→SPN and GP→NSt responses during STD used a nonhydrolyzable selective agonist, quinelorane (1 μM) (see *SI Text*). Fig. 4 shows that STD was reduced for both SPN→SPN (n = 2 of 3 pair recordings) and GP→NSt (n = 9 of 11 population recordings) responses [n = 11

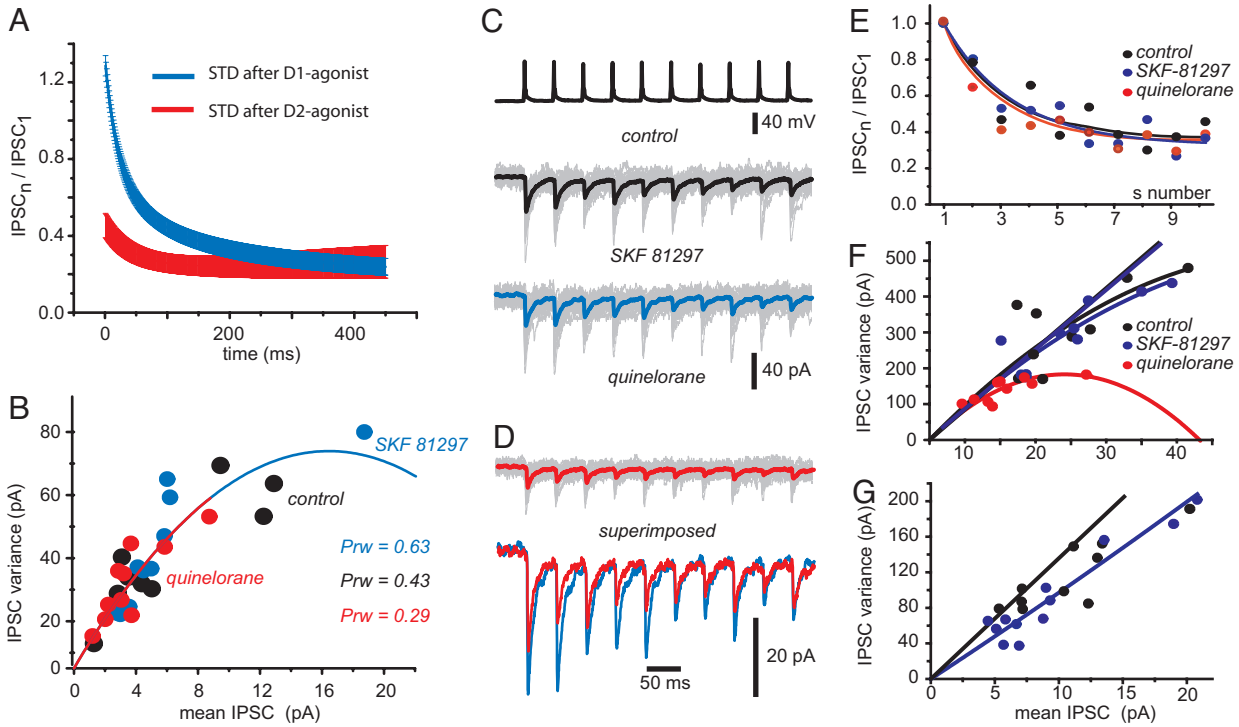

Fig. 5. Modulation is different for interneurons. (*A*) Summary plot of all responsive synapses interconnecting SPNs comparing STD kinetics after the D_1-class agonist (blue) and D_2-class agonist (red) (mean ± SEM). Plots show the lower and upper limits of dopamine-induced STD variation for synapses interconnecting SPNs. (*B*) Variance-mean analysis in one SPN→SPN connection that responded to both D_1- and D_2-agonists. If all points are fitted to one parabola (see *SI Text*), D_1-action increases and D_2-action decreases release probability. (*C*) FS→SPN connection. (*Top*) Presynaptic APs from an FS interneuron evoked IPSCs from a postsynaptic SPN in the control (black) after adding SKF-81297 (1 μM) (blue) (*Middle*) and after adding quinelorane (1 μM) (red) (*Bottom*). Note that SKF-81297 had no effects, but quinelorane did. (*D*) Last two traces (after D_1- and D_2-agonists) are shown expanded and superimposed. Quinelorane had a clear action: Most IPSCs were reduced. (*E*) However, there was no change in STD kinetics after any dopamine agonist. (*F*) Variance-mean analysis of the same FS→SPN connection. The change in initial plot after quinelorane was not significant. (*G*) In the FS→SPN connection, responsive to the D_1-agonist, there was a change in initial slope after variance-mean analysis.

of 14 (78%) cases responded to D_2-agonist]. The results were pooled together to obtain the change in STD ratio induced by the D_2-agonist, from 4.5 ± 0.6 before to 2.7 ± 0.4 after quinelorane ($n = 11$; $P < 0.008$). Although some cases did not respond, responsive cases are more than expected by the receptor segregation hypothesis into two pathways (49, 50). A decrease in STD corresponded to a decrease in $IPSC_1$ from 94 ± 25 pA before to 45 ± 13 pA after the D_2-agonist ($n = 11$; $P < 0.005$). To see whether this change was due to presynaptic mechanisms, the CV of $IPSC_1$ was assessed. It was significantly enhanced (220 ± 40%) ($P < 0.008$), suggesting a presynaptic mechanism (32). In addition, IPSC variance was significantly decreased ($P \leq 0.05$; $n = 11$; F test) in each responsive experiment, and τ_1 of the STD process increased significantly from 31 ± 2 to 42 ± 4 msec ($P < 0.03$), suggesting synaptic "redistribution" (4, 8, 48). While using quinelorane, special care was taken to discard cases showing signs of long-term depression after repeated trains. These effects were completely blocked by the selective $D_{2/3}$-class antagonist, sulpiride (1 μM) ($n = 4$; data not shown).

Fig. 5*A* illustrates means ± SEM of fitted exponential functions (see *Materials and Methods*) for STD processes after normalizing and averaging all responsive cases (SKF 81297, blue; quinelorane, red). The limits of STD change for synapses between SPNs are then illustrated. Significant differences are restricted to the initial part of the process and are not evident during the last IPSCs in the train. This plot is typical of synaptic redistribution (4, 8, 48).

Although several cases were unresponsive to a given agonist, it was possible to obtain a response for both agonists, administered in sequence, in two unitary connections (SPN→SPN) ($n =$ 2 of 2). We took advantage from such cases to perform variance-mean analysis (Fig. 5*B*) (14, 47). Fig. 5*B* shows superimposed parabolas fitted to the data points from different conditions (32, 42). The result suggested a larger release probability after the D_1-agonist than after the D_2-agonist, in agreement with the changes in CV (Fig. 2*B*) (45) and the hypothesis of synaptic redistribution (Fig. 5*A*) (4, 8, 48). However, as in other cases, intrinsic quantal variability associated with unitary connections, and other factors, impeded a precise distinction between N (release sites) and P (release probability) (41, 51). However, both parameters signal presynaptic mechanisms. In contrast, the constancy of quantal amplitude excludes postsynaptic mechanisms (see *SI Text*).

Taken together, the results show that the dopaminergic system may modulate the STD of synapses that interconnect spiny neurons. D_1-class receptors enhance STD, whereas D_2-class receptors decrease STD by activating presynaptic receptors.

Modulation of Synapses Between FS Interneurons and Spiny Neurons. The STD of FS→SPN connections was investigated with dual recordings and selective dopamine agonists. The D_1-class selective agonist, SKF-81297 (1 μM), enhanced unitary IPSCs ($n =$ 1 of 4 pair recordings), whereas the D_2-class selective agonist, quinelorane (1 μM), decreased unitary IPSCs ($n = 3$ of 4 pair recordings). Three FS→ SPN connections showed a response to quinelorane ($n = 3$), with an average $IPSC_1$ reduction of 66 ± 1%. A representative case is illustrated in Fig. 5*C*. This connection was unresponsive to SKF-81297. FS interneurons unresponsive to both agonists were frequently found (32). Despite a clear modulation of synaptic strength in responsive cases (Fig. 5*D*),

quinelorane did not change STD (Fig. 5*E*). STD ratios were 2.7 ± 4 before and 2.6 ± 0.5 after the D_2-agonist in responsive cases. Variance-mean analysis (Fig. 5*F*) showed no significant change in initial slope of parabolas despite changes in amplitude and variance. Thus, FS synapses exhibit presynaptic modulation of synaptic strength, but no signs of STD modulation (52) (see *Discussion*).

In a case responsive to the D_1-agonist, IPSC amplitude increased 159% (data not shown). This action did not interfere with STD kinetics. Variance-mean analysis (Fig. 5*G*) suggested that this action was postsynaptic (53). However, it coursed with a decrease in quantal amplitude (54), implying, perhaps, a mixture of pre- and postsynaptic actions.

Discussion

The basis for the selection and organization of motor synergies may depend on the lateral inhibition between SPNs (12, 14, 18, 20–23, 25). The present work demonstrates that this lateral inhibition exhibits STD that can be modulated by the dopamine system. STD is in charge of controlling the gain and filtering capabilities of a circuit to increase its sensitivity to sudden changes (4–7, 9, 10, 48). Hence, fast selection of motor synergies may depend on dopaminergic modulation of STD between SPNs. Patients with Parkinson's disease have problems beginning or changing motor tasks.

It was shown that STD exhibited by the inhibitory synapses that interconnect SPNs (13, 14) can be enhanced by the activation of D_1-class receptors. This change would make the circuit suitable to respond to sudden fast commands (48) and subtle changes in frequency (dynamic component), helping to balance inputs of different strengths (6, 9, 39). However, D_2-class receptors decrease STD, perhaps setting the circuit to keep responding to and transferring a continuous basal level of activity (static or tonic component) (6, 9, 39). STD modulation was demonstrated by dual (unitary) recordings between SPNs and by field stimulation of groups of afferents arising from striofugal axons stimulated at the GP. Some synaptic responses did not respond to a given applied agonist, suggesting that not all terminals have both receptor classes (49, 50). If terminals had dopamine receptors segregated, it can be hypothesized that the direct pathway is the structural basis for the dynamic component, whereas the indirect pathway is the platform for the static component. Both pathways would complement each other (12, 33, 35), e.g., different sets of coordinated muscles may be appointed to fast actions (dynamic component), whereas others may be needed to preserve tone and posture (static component). Interestingly, D_2-class receptors have more affinity for dopamine than D_1-class receptors (see *SI Text*) (55). This difference in affinity suggests that D_2-class receptors maintain a dopaminergic tone with low basal dopamine concentrations, whereas D_1-class receptors respond during sudden peaks in dopamine concentration (56, 57), suggesting that affinities of receptors for dopamine are in agreement with the role that these receptors play in synaptic function. It reinforces the view that D_2 and D_1 actions represent the static and dynamic branches of the same system.

Nonetheless, some unitary connections responded to both D_1- and D_2-class agonists, suggesting a degree of colocalization (58–60). Hence, some sets of terminals may shift their plasticity between the lowest and highest degrees of STD. This intersection between pathways (59) may quickly change the balance between dynamic and tonic neurons depending on the context.

Another target for dopamine in the NSt are the interneurons and their synapses (14, 26, 27, 29–32, 61, 62). Dopamine agonists depolarize FS interneurons in the striatum by D_1-class receptors (61). However, in most cases, we did not observe a presynaptic modulation by the D_1-agonist (FS→SPN) (32). We only found an enhancement of IPSCs in one of four (25%) FS→SPN connections treated with SKF-81297 (1 μM). Variance-mean analysis indicated a change in initial slope in this case (Fig. 5*G*) (53, 54), suggesting postsynaptic mechanisms.

A reduction of IPSCs was found in three of four (75%) FS→SPN connections treated with quinelorane (62) (Fig. 5 *C–F*). Noticeably, STD was not changed. Presynaptic inhibition without STD changes has been seen in other synapses (52, 63, 64). The mechanism proposed to dissociate presynaptic modulation of synaptic strength from modulation of STD includes the presence of some proteins such as parvalbumin or calcium sensors (65, 66).

Therefore, the dopamine system may affect presynaptically some interneurons but not others, suggesting heterogeneity of interneuron types (32, 67); these presynaptic actions do not imply STD modulation. It is concluded that SPN→SPN synapses can transiently modify their strength and computational properties, whereas FS→SPN synapses can only modify their strength. This difference may serve to rearrange the balance among different types of inhibition.

STP mainly depends on presynaptic mechanisms such as release probability and refilling rate of the vesicle pool (48). Calcium dynamics reflects the "use" or "history" of network activity (1–5, 68). Therefore, presynaptic receptors can be conceived as sensors and regulators of the dynamics and computational properties of circuits, not simply as modifiers of synaptic strength (32, 41, 69, 70).

Materials and Methods

Electrophysiology. Electrophysiological experiments were performed by using neostriatal slices (250–300 μm thick) from Wistar rats PD19–PD22 cut in 4°C saline by using a vibratome (Ted Pella, Reading, CA) as described previously (32). For a more detailed account on methods, see *SI Text*. Extracellular saline containing (in mM) 126 NaCl, 3 KCl, 1 $MgCl_2$, 2 $CaCl_2$, 26 $NaHCO_3$, and 10 glucose (pH 7.4 with NaOH, 298 mOsm/liter with glucose, saturated with 95% O_2 and 5% CO_2; 25–27°C). 6-cyano-2,3-dihydroxy-7-nitro-quinoxaline disodium salt (CNQX) (10 μM) and D-(-)-2-amino-5 phosphonovaleric acid (AP5) (50 μM) were added to block AMPA and NMDA receptors, respectively. Standard whole-cell recordings using infrared differential interference contrast (IR-DIC) microscopy with an upright microscope and a digital camera were used to obtain IPSCs with the help of an Axoclamp 2B and/or Axopatch 200B amplifiers (Axon Instruments, Foster City, CA). Traces shown are the average of 4-min recordings (24 traces) taken when the amplitude had been stabilized for a given condition. IPSCs were evoked by field stimulation using a bipolar electrode located at the GP (32). The intracellular saline for postsynaptic medium spiny neurons contained (in mM) 72 KH_2PO_4, 36 KCl, 2 $MgCl_2$, 10 Hepes, 1.1 EGTA, 0.2 Na_2ATP, 0.2 Na_3GTP, 5 QX-314, and 1% biocytin (pH 7.2)/275 mOsm/liter for a theoretical $E_{Cl^-} = -30$ mV. Experiments were performed at 25°C to 27°C. Series resistances ranged from 5 to 20 MΩ and were partially compensated (60–90%). Whole-cell recordings of postsynaptic medium SPNs were recorded in voltage-clamp mode at a holding potential of −85 mV. Postsynaptic cells were located in the vicinity (<100 μm) of a presynaptic SPN or FS neuron recorded in current-clamp mode. The presynaptic neuron was stimulated with brief current pulses that evoked action potentials (1–5 msec, 0.2–0.3 nA). Single stimuli or trains of 10 stimuli were evoked at a frequency of 10, 20, or 50 Hz every 10 sec. Digitized data were saved on a disk and analyzed with commercial software (Origin version 7; Microcal, Northampton, MA). IPSC amplitudes were measured from basal line to peak for the first response in a train ($IPSC_1$). For the subsequent responses ($IPSC_n$), the basal line remaining from the previous response was subtracted. Distribution-free statistical procedures (Systat version 11; SPSS, Chicago, IL) were used to find data significance.

Amplitudes of IPSCs in a train were fitted to a sum of exponential functions after normalization:

$$\mathrm{IPSC}(t) = A_1 e^{-x/\tau 1} + A_2 e^{-x/\tau 2} + y0. \quad [1]$$

Fast (τ_1) and slow (τ_2) time constants of decay are obtained from this fit (48). A_1 and A_2 are the magnitude of the postsynaptic response for each exponential component, and *y0* represents residual baseline activity. We measured the STD ratio as $\mathrm{IPSC}_1/\mathrm{IPSC}_{7-10}$. Variance-mean analysis was performed as proposed by Clements and Silver (2000), and the details are provided in *SI Text*.

Pharmacology. Drugs were dissolved in the bath saline from stock solutions made daily and were administered by using a gravity-driven superfusion system. Equilibrated concentrations of the drugs were achieved in 4 to 5 min. All of the following were purchased from Sigma–Aldrich (St. Louis, MO): CNQX, AP5, L-glutamic acid [glutamate (GLU)], SKF 81297, SCH 23390, bicuculline, QX-314, and quinelorane.

Immunohistochemistry. Neurons were filled with biocytin during recording. Slices with a single or two filled neurons (paired recordings) were taken into consideration for immunocytochemistry. A combination of intracellular labeling and substance P, enkephalin, or parvalbumin immunocytochemistry was used in each occasion to identify the recorded neurons (28, 32). Details of the methods can be found elsewhere (32), and a brief summary is given in *SI Text*.

We thank D. Tapia and A. Laville for technical support. This work was supported by IMPULSA-Universidad Nacional Autónoma de México and Dirección General de Asuntos del Personal Académico-Universidad Nacional Autónoma de México grants (to J.B. and E.G.) and Consejo Nacional de Ciencia y Tecnología-Mexico Grants 42636 (to E.G.) and 49484 (to J.B.).

1. Zucker RS, Regehr WG (2002) *Ann Rev Physiol* 64:355–405.
2. Abbott LF, Nelson SB (2000) *Nat Neurosci* 3:1178–1183.
3. Thomson AM (2000) *Trends Neurosci* 23:305–312.
4. Abbott LF, Regehr WG (2004) *Nature* 431:796–803.
5. Thomson AM (2000) *Prog Neurobiol* 62:159–196.
6. Richardson MJ, Melamed O, Silberberg G, Gerstner W, Markram H (2005) *J Comput Neurosci* 18:323–331.
7. Fuhrmann G, Segev I, Markram H, Tsodyks M (2002) *J Neurophysiol* 87:140–148.
8. Markram H, Tsodyks M (1996) *Nature* 382:807–810.
9. Abbott LF, Varela JA, Sen K, Nelson SB (1997) *Science* 275:220–224.
10. O'Donovan MJ, Rinzel J (1997) *Trends Neurosci* 20:431–433.
11. Czubayko U, Plenz D (2002) *Proc Natl Acad Sci USA* 99:15764–15769.
12. Groves PM (1983) *Brain Res* 286:109–132.
13. Gustafson N, Gireesh-Dharmaraj E, Czubayko U, Blackwell KT, Plenz D (2006) *J Neurophysiol* 95:737–752.
14. Koos T, Tepper JM, Wilson CJ (2004) *J Neurosci* 24:7916–7922.
15. Park MR, Lighthall JW, Kitai ST (1980) *Brain Res* 194:359–369.
16. Taverna S, van Dongen YC, Groenewegen HJ, Pennartz CM (2004) *J Neurophysiol* 91:1111–1121.
17. Tunstall MJ, Oorschot DE, Kean A, Wickens JR (2002) *J Neurophysiol* 88:1263–1269.
18. Venance L, Glowinski J, Giaume C (2004) *J Physiol* 559:215–230.
19. Wickens JR, Alexander ME, Miller R (1991) *Synapse* 8:1–12.
20. Wickens JR, Oorchcot DE (2000) in *Brain Dynamics and the Striatal Complex*, eds Miller R, Wickens JR (Harwood, Australia), pp 141–150.
21. Bar-Gad I, Bergman H (2001) *Curr Opin Neurobiol* 11:689–695.
22. Plenz D (2003) *Trends Neurosci* 26:436–443.
23. Latash ML, Shim JK, Smilga AV, Zatsiorsky VM (2005) *Biol Cyber* 92:186–191.
24. Nicola SM, Woodward Hopf F, Hjelmstad GO (2004) *Cell Tissue Res* 318:93–106.
25. Sil'kis IG (2006) *Neurosci Behav Physiol* 36:631–643.
26. Kita H (1993) *Prog Brain Res* 99:51–72.
27. Bennett BD, Bolam JP (1994) *Neuroscience* 62:707–719.
28. Koos T, Tepper JM (1999) *Nat Neurosci* 2:467–472.
29. Tepper JM, Bolam JP (2004) *Curr Opin Neurobiol* 14:685–692.
30. Tepper JM, Koos T, Wilson CJ (2004) *Trends Neurosci* 27:662–669.
31. Tepper JM, Plenz D (2005) in *The Interface between Neurons and Global Brain Function*, *Dahlem Workshop Report* 93, eds Grillner S, Graybiel AM (MIT Press, Cambridge, MA), pp 127–148.
32. Guzman JN, Hernandez A, Galarraga E, Tapia D, Laville A, Vergara R, Aceves J, Bargas J (2003) *J Neurosci* 23:8931–8940.
33. Albin RL, Young AB, Penney JB (1995) *Trends Neurosci* 18:63–64.
34. Hornykiewicz O (1973) *Br Med Bull* 29:172–178.
35. Wichmann T, DeLong MR (2003) *Ann NY Acad Sci* 991:199–213.
36. Wooten GF (1990) in *Neurobiology of Disease*, ed Pearlman AL (Oxford, Univ Press, New York), pp 454–468.
37. Hernandez-Lopez S, Bargas J, Surmeier DJ, Reyes A, Galarraga E (1997) *J Neurosci* 17:3334–3342.
38. Hernandez-Lopez S, Tkatch T, Perez-Garci E, Galarraga E, Bargas J, Hamm H, Surmeier DJ (2000) *J Neurosci* 20:8987–8995.
39. Silberberg G, Wu C, Markram H (2004) *J Physiol* 556:19–27.
40. Perez-Rosello T, Figueroa A, Salgado H, Vilchis C, Tecuapetla F, Guzman JN, Galarraga E, Bargas J (2005) *J Neurophysiol* 93:2507–2519.
41. Salgado H, Tecuapetla F, Perez-Rosello T, Perez-Burgos A, Perez-Garci E, Galarraga E, Bargas J (2005) *J Neurophysiol* 94:3771–3787.
42. Tecuapetla F, Carrillo-Reid L, Guzman JN, Galarraga E, Bargas J (2005) *J Neurophysiol* 93:1119–1126.
43. Romo R, Scarnati E, Schultz W (1992) *Exp Brain Res* 91:385–395.
44. Stern EA, Kincaid AE, Wilson CJ (1997) *J Neurophysiol* 77:1697–1715.
45. Silver RA, Momiyama A, Cull-Candy SG (1998) *J Physiol* 510:881–902.
46. Koos T, Tepper JM (2002) *J Neurosci* 22:529–535.
47. Clements JD, Silver RA (2000) *Trends Neurosci* 23:105–113.
48. Tsodyks MV, Markram H (1997) *Proc Natl Acad Sci USA* 94:719–723.
49. Gerfen CR (2000) *Ann Neurol* 47:S42–S50.
50. Gerfen CR, Engber TM, Mahan LC, Susel Z, Chase TN, Monsma FJ, Jr, Sibley DR (1990) *Science* 250:1429–1432.
51. Biro AA, Holderith NB, Nusser Z (2006) *J Neurosci* 26:12487–12496.
52. Hefft S, Kraushaar U, Geiger JR, Jonas P (2002) *J Physiol* 539:201–208.
53. Flores-Hernandez J, Hernandez S, Snyder GL, Yan Z, Fienberg AA, Moss SJ, Greengard P, Surmeier DJ (2000) *J Neurophysiol* 83:2996–3004.
54. Gonzalez-Islas C, Hablitz JJ (2001) *J Neurophysiol* 86:2911–2918.
55. Missale C, Nash SR, Robinson SW, Jaber M, Caron MG (1998) *Physiol Rev* 78:189–225.
56. Giros B, Jaber M, Jones SR, Wightman RM, Caron MG (1996) *Nature* 379:606–612.
57. Suaud-Chagny MF, Dugast C, Chergui K, Msghina M, Gonon F (1995) *J Neurochem* 65:2603–2611.
58. Surmeier DJ, Song WJ, Yan Z (1996) *J Neurosci* 16:6579–6591.
59. Deng YP, Lei WL, Reiner A (2006) *J Chem Neuroanat* 32:101–116.
60. Mizuno T, Schmauss C, Rayport S (2007) *BMC Neurosci* 8:8.
61. Bracci E, Centonze D, Bernardi G, Calabresi P (2002) *J Neurophysiol* 87:2190–2194.
62. Delgado A, Sierra A, Querejeta E, Valdiosera RF, Aceves J (2000) *Neuroscience* 95:1043–1048.
63. Hefft S, Jonas P (2005) *Nat Neurosci* 8:1319–1328.
64. Hjelmstad GO (2004) *J Neurosci* 24:8621–8628.
65. Sippy T, Cruz-Martin A, Jeromin A, Schweizer FE (2003) *Nat Neurosci* 6:1031–1038.
66. Caillard O, Moreno H, Schwaller B, Llano I, Celio MR, Marty A (2000) *Proc Natl Acad Sci USA* 97:13372–13377.
67. Gao WJ, Wang Y, Goldman-Rakic PS (2003) *J Neurosci* 23:1622–1630.
68. Brenowitz S, Trussell LO (2001) *J Neurosci* 21:1857–1867.
69. Selig DK, Nicoll RA, Malenka RC (1999) *J Neurosci* 19:1236–1246.
70. Wilson RI, Nicoll RA (2001) *Nature* 410:588–592.